



Asian Journal of Chemistry; Vol. 26, No. 14 (2014), 4423-4426

ASIAN JOURNAL OF CHEMISTRY

<http://dx.doi.org/10.14233/ajchem.2014.16779>



Preparation of SrBi₂O₄/Ti Anode and Its Photocatalytic and Photoelectrochemical Oxidation Performance

GUOTING LI, ZHAO YE and LINGFENG ZHU*

Institute of Environmental and Municipal Engineering, North China University of Water Resources and Electric Power, Zhengzhou 450011, P.R. China

*Corresponding author: Tel/Fax: +86 371 65790239; E-mail: zhulingfengzy@ncwu.edu.cn

Received: 28 November 2013;

Accepted: 20 February 2014;

Published online: 5 July 2014;

AJC-15488

DSA anode SrBi₂O₄/Ti is prepared and used for photocatalytic and photoelectrochemical oxidation of azo dye Orange II. SrBi₂O₄ is tentatively immobilized onto H₂C₂O₄ treated Ti substrate by dip-coating of SrBi₂O₄ precursor solution. Subsequent calcination of the immobilized Ti substrate at 700 °C for 2 h could produce SrBi₂O₄/Ti anode. The surface pore structure of H₂C₂O₄ treated Ti substrate facilitates the combination between SrBi₂O₄ crystals and Ti substrate by SEM analysis. The average diameter of SrBi₂O₄ crystals is within 5 μm and they are compactly combined with each other. The component and crystal structure of SrBi₂O₄ are also confirmed by EDX and XRD analysis. Under the irradiation from Xenon lamp (with UV-cutoff filter), tungsten lamp and ultraviolet lamp, the Orange II decolorization efficiency by photoelectrochemical oxidation is significantly higher than those by photocatalytic oxidation and electrochemical oxidation alone. Meanwhile, the synergetic factor *f* under tungsten lamp irradiation achieves 239.5 %, which is more significant than under visible and ultraviolet irradiation. Both the wavelength of light source and the proportion between visible light and ultraviolet are proved to be fundamental for the photoelectrochemical process.

Keywords: SrBi₂O₄, Anode, Photocatalytic oxidation, Electrochemical oxidation, Photoelectrochemical oxidation.

INTRODUCTION

Advanced oxidation processes (AOPs) are all characterized by the production and utilization of HO• radicals (2.72 V/NHE), which are the most reactive radicals in aqueous solution¹. Pathogenic organisms could be efficiently killed by the oxidizing species produced by AOPs^{2,3}. A number of organic pollutants, particularly toxic and refractory pollutants, can be degraded effectively and even mineralized to carbon oxide, water and inorganics if the reaction time was prolonged⁴⁻⁷. Due to the wide application, AOPs are currently receiving the ever-increasing concern around the world.

Among advanced oxidation processes, photocatalytic oxidation and electrochemical oxidation processes are especially interesting as they can be integrated to be photoelectrochemical oxidation process. In terms of photocatalytic oxidation, the recombination of charge carriers on semiconductors could result in low quantum efficiency and poor degradation performance⁸. For electrochemical oxidation, partial degradation of aromatics could lead to the accumulation of intermediates with higher toxicity than their parent molecules, which is attributed to the insufficient generation of oxidizing species⁹⁻¹¹. By application of an external electric field on an anode with photocatalytic activity, charge carriers can be effectively separated in

photocatalytic oxidation process. Meanwhile, the enhanced photocatalytic oxidation efficiency could help to produce more oxidizing species for organics degradation. A synergetic effect was always observed in photoelectrochemical oxidation process^{6,12}. Accordingly, photoelectrochemical oxidation is a promising technology for organics degradation in water and wastewater purification.

For photocatalytic oxidation and electrochemical oxidation processes, catalytic materials play the key role as the reaction efficiency is highly dependent on the type of catalytic material. Therefore, the selection of anode material for photoelectrochemical oxidation is considered to be vital for the total performance. On the other hand, the light source is also fundamental for the degradation efficiency. Ultraviolet irradiation consists of only about 5 % of total solar energy, while visible light accounts for as much as 45 %. The utilization of both ultraviolet and visible light in photoelectro-chemical oxidation process seems to be more important from a practical point of view.

In this research, SrBi₂O₄, a visible light active catalyst^{13,14}, is tentatively immobilized onto a H₂C₂O₄ treated Ti substrate. The prepared anode SrBi₂O₄/Ti is used in the photocatalytic oxidation, electrochemical oxidation and photoelectrochemical oxidation of an azo dye Orange II. Xenon lamp (with UV-

cutoff filter), tungsten lamp and ultraviolet lamp are employed to provide visible light, simulated solar light and ultraviolet irradiation to explore the degradation performance.

EXPERIMENTAL

Orange II was purchased from the Beijing Chemical Reagents Company and used without further purification. Other chemicals used were of analytical-reagent grade. The titanium substrate (40 × 50 mm) was provided by the Beijing Titanium Industrial and Trade Company. Visible light irradiation was provided by a 150 W Xenon lamp (Zhuolihanguang Instrument Corporation, Ltd., Beijing, China) with a UV cut-off filter to remove the light with wavelength shorter than 400 nm. A 15 W UV lamp (Aosilan Instrument Corporation, Ltd., Wenzhou, China) with a maximum emission at 254 nm was used to provide the ultraviolet irradiation. A commercially available 100 W tungsten lamp was employed to simulate solar light irradiation.

Preparation of SrBi₂O₄/Ti anode: Pretreatment of the titanium substrate surface (40 × 50 mm) was carried out following the procedures suggested by Feng and Johnson¹⁵. The mesh was degreased with 40 % NaOH solution. Then it was immersed in a boiling aqueous solution of H₂C₂O₄ (15 %) until TiO₂ dissolved, producing grey titanium substrate.

The precursor solution was prepared by mixing Bi(NO₃)₃·5H₂O, Sr(NO₃)₂, HNO₃, citric acid and glycol with a desired proportion. Initially, certain amount of Bi(NO₃)₃·5H₂O was added into dilute HNO₃ solution until Bi(NO₃)₃·5H₂O was completely dissolved. Subsequently, Sr(NO₃)₂, glycol and citric acid were sequentially added in the above aqueous solution, in which the molar ratio between Sr(NO₃)₂ and Bi(NO₃)₃ was maintained at 1:2. The mixture was kept stirring for 2-3 h and a transparent precursor solution was obtained.

The H₂C₂O₄ treated titanium substrate was dipped in the precursor solution. After being taken out of the mixture, the

titanium substrate was dried in an oven at 120 °C for 0.5 h. The thickness of the film was controlled by the repeated times of dip coating procedure. Then the titanium substrate was heated at 700 °C in a muffle furnace for 2 h and SrBi₂O₄/Ti anode was prepared. H₂C₂O₄ treated Ti substrate was also calcined in the muffle furnace with same procedures.

Characterization: The morphologies of titanium substrate and SrBi₂O₄/Ti anode were recorded on a Philips Quanta-2000 scanning microscope coupled with an energy dispersive X-ray (EDX) spectrometer. The X-ray diffraction (XRD) patterns of SrBi₂O₄/Ti and the thermally treated Ti substrate were recorded on a Rigaku D/MAX-3B X-diffractometer.

Degradation of orange II by photocatalytic oxidation, electrochemical oxidation and photoelectrochemical oxidation: These reactions were carried out in a semi-cylindrical quartz reactor. Titanium wire was used as cathode and the prepared SrBi₂O₄/Ti anode was employed. The available volume of the reactor was 150 and 125 mL Orange II (20 mg/L) solution was added. Irradiations from 150 W Xenon lamp (with UV-cutoff filter), 100 W tungsten lamp and 15 W UV lamp was applied on the prepared SrBi₂O₄/Ti anode. The lamps were situated parallel to the anode tested at a distance of 30 mm from the quartz reactor.

Analyses: An UVmini 1240 UV-visible spectrophotometer (Shimadzu, Japan) was employed to measure the concentration of Orange II samples at 484 nm, which corresponded to the maximum absorption of the dye.

RESULTS AND DISCUSSION

Surface morphologies of raw Ti substrate, H₂C₂O₄ treated Ti substrate SrBi₂O₄/Ti anode: SEM images of raw Ti substrate, H₂C₂O₄ treated Ti substrate and SrBi₂O₄/Ti anode are presented in Fig.1. Apparently, compared with the smooth raw Ti substrate in Fig.1 a and b, many pores and honey-comb

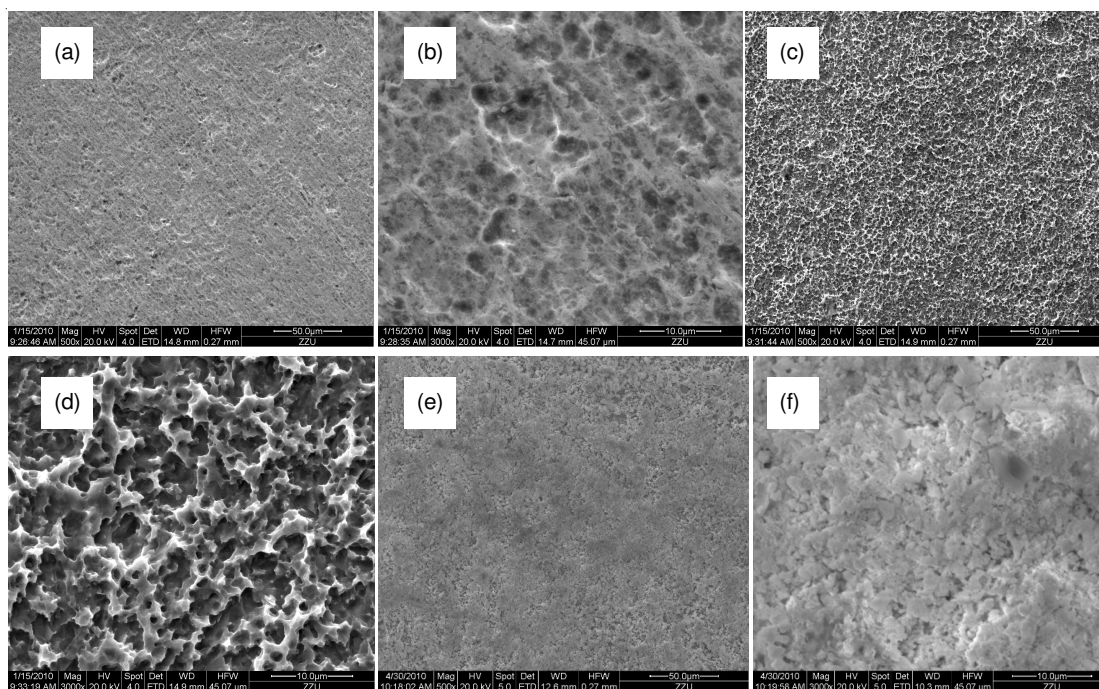


Fig. 1. SEM micrographs of raw Ti substrate (a,b), H₂C₂O₄ treated Ti substrate (c,d), and SrBi₂O₄/Ti anode (e,f). (a), (c) and (e) are magnified 500 times while (b), (d) and (f) are magnified 3000 times

structures are generated on the Ti substrate after chemical etching in boiling H₂C₂O₄ solution. As illustrated in Fig. 1 c and d, the average diameter of these pores is within 10 μm and they are compactly distributed on the anode surface, which is consistent with previous study¹⁶. Meanwhile, the rough surface of the H₂C₂O₄ treated Ti substrate is expected to facilitate the immobilization of SrBi₂O₄ crystals. As a comparison, in Fig. 1 e and f, SrBi₂O₄ crystals have been immobilized onto the Ti substrate. The pore structures on the H₂C₂O₄ treated Ti substrate are occupied by the SrBi₂O₄ crystals, indicating a good combination between SrBi₂O₄ crystals and Ti substrate. The SrBi₂O₄ crystals are observed to be evenly distributed on the anode surface. The average diameter of these crystals is within 5 μm and they are compactly combined with each other as well.

The EDX microanalysis of SrBi₂O₄/Ti electrode was also conducted to further confirm the existence of SrBi₂O₄ coating, as presented in Fig. 2. The molar ratios of Sr and Bi are 9.2 and 12.5 %, respectively. The main elements for the SrBi₂O₄/Ti are Sr, Bi, Ti and O. The coexistence of TiO₂ indicates that the thickness of the SrBi₂O₄ coating is not thick enough to cover the Ti substrate totally. Consequently, TiO₂ can be formed concurrently after calcination at 700 °C in a muffle furnace.

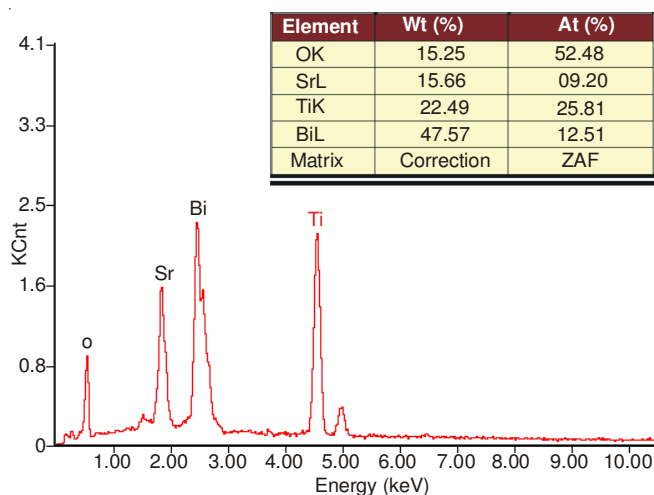


Fig. 2. EDX graph of SrBi₂O₄/Ti anode

XRD of SrBi₂O₄/Ti anode: XRD patterns of SrBi₂O₄/Ti anode and thermally treated Ti substrate are illustrated in Fig. 3. Obviously, SrBi₂O₄/Ti anode shares all the diffraction peaks which are attributed to the thermally treated Ti substrate.

It indicates that the anode surface is not completely covered by SrBi₂O₄, which is consistent with the aforementioned EDX results. On the other hand, the other peaks except that of the thermally treated Ti substrate c are attributed to SrBi₂O₄.

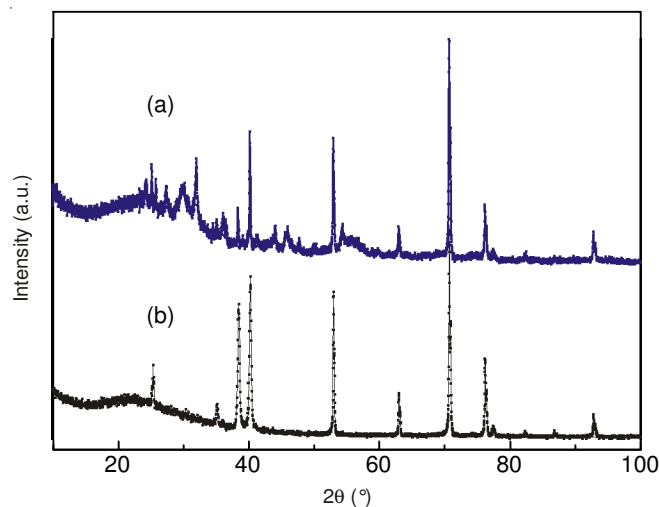


Fig. 3. XRD patterns of SrBi₂O₄/Ti anode (a) and thermally treated Ti substrate (b)

Photocatalytic and photoelectrochemical performance under different lamp source irradiation:

Three processes including photocatalytic oxidation (PO), electrochemical oxidation (EO) and photoelectrochemical oxidation process (PE) are employed to explore the performance of the prepared SrBi₂O₄/Ti anode. Irradiation from Xenon lamp (with UV-cutoff filter), tungsten lamp and ultraviolet lamp are compared during the degradation, which is presented in Fig. 4. The current under 1.5 V potential was not detected using an amperometer as no electrolyte was introduced in the Orange II solution. As a result, the effect of electrochemical oxidation is apparently insignificant as the removal efficiency only achieves 1.3 %. Regarding the photocatalytic oxidation process, the removal efficiencies under visible light (Xenon lamp with UV-cutoff filter), tungsten lamp and ultraviolet irradiation reaches 1.0, 1.5 and 28.6 %, respectively. This implies that the irradiation wavelength plays the predominant role for photocatalytic oxidation of Orange II using the prepared anode. In addition, the removal efficiencies of photoelectrochemical process are the highest among the three processes. Particularly under

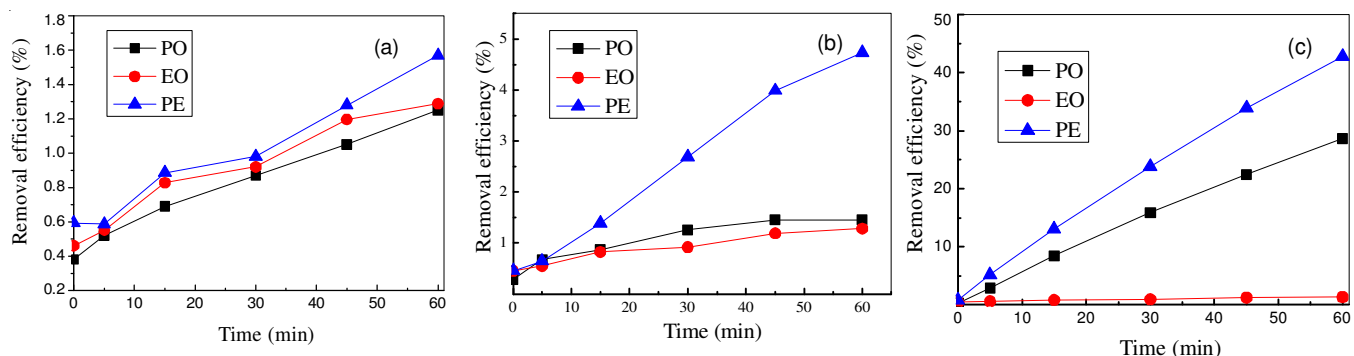


Fig. 4. Decolorization of Orange II by photocatalytic oxidation (PO), electrochemical oxidation (EO) and photoelectrochemical process (PE) under Xenon lamp (with UV-cutoff filter) (a), tungsten lamp (b) and ultraviolet irradiation (c)

tungsten lamp irradiation, the efficiency of photoelectrochemical process is obviously higher than other two processes.

Synergetic effect during photocatalytic and photoelectrochemical degradation process: For photocatalytic oxidation, electrochemical oxidation and photoelectro-chemical oxidation processes, the degradation processes can be well followed by pseudo-first-order reaction model. The correlation between $\ln(C_0/C)$ and reaction time is linear. The kinetic expression can be presented as follows:

$$\ln(C_0/C) = k_{app} t \quad (1)$$

where C_0 is the initial Orange II concentration, C is the Orange II concentration at instant t , k_{app} (min^{-1}) is the apparent rate constant of pseudo-first-order reaction and ' t ' is the time of reaction.

Due to the especially low reaction rate under visible light irradiation, the k_{app} for the three processes are very close and insignificant. Herein, only the k_{app} values under tungsten lamp and ultraviolet irradiation are presented in Table-1. The k_{app} in photoelectrochemical oxidation process under tungsten lamp and ultraviolet irradiation achieves 7.73×10^{-4} and 0.0092 min^{-1} , respectively. It is obvious that ultraviolet irradiation is more powerful than tungsten lamp and ultraviolet irradiation in both photocatalytic oxidation and photoelectrochemical oxidation processes.

TABLE-1
REACTION RATE CONSTANTS (k_{app}) UNDER
TUNGSTEN LAMP AND ULTRAVIOLET IRRADIATION

Irradiation		PO	EO	PE
Tungsten lamp	k_{app} (min^{-1})	1.46×10^{-4}	8.12×10^{-5}	7.73×10^{-4}
	R^2	0.960	0.994	0.997
Ultraviolet lamp	k_{app} (min^{-1})	0.00559	8.12×10^{-5}	0.0092
	R^2	0.999	0.994	0.999

As we know, photocatalytic oxidation could be enhanced significantly by the application of an external electric field, which is called photoelectrochemical process¹⁷. A synergetic effect may be observed for the integrated process. In order to clearly indicate the synergetic effect, synergetic factor (f) is introduced as following¹⁸:

$$f = [k_{PE} / (k_{PO} + k_{EO}) - 1] \times 100 \% \quad (2)$$

where k_{PE} is the k_{app} for photoelectrochemical oxidation process, k_{PO} is k_{app} for photocatalytic oxidation process and k_{EO} is k_{app} for electrochemical oxidation process.

The resulted synergetic factors showed in Table-2. The higher the ' f ' value is, the more significant the synergetic effect. It can be observed that the ' f ' value under tungsten lamp irradiation achieves 239.5 %, which is much higher than that under ultraviolet irradiation. Compared with the overall ultraviolet irradiation, only a small part of ultraviolet irradiation can be detected in the tungsten lamp irradiation. Even though, the synergetic effect is still considerable for tungsten lamp irradiation. The above indicates that both the wavelength of the light source and the proportion between visible light and ultraviolet are fundamental for the photoelectrochemical process.

TABLE-2
VALUE OF f UNDER TUNGSTEN AND
ULTRAVIOLET LAMP IRRADIATION

Irradiation	Tungsten lamp	Ultraviolet lamp
f	239.5 %	62.2 %

Conclusion

$\text{SrBi}_2\text{O}_4/\text{Ti}$ anode is prepared by dip-coating of SrBi_2O_4 precursor solution onto $\text{H}_2\text{C}_2\text{O}_4$ treated Ti substrate and subsequent calcination procedure. The surface compact SrBi_2O_4 crystals have a good combination with Ti substrate. The component and crystal structure of SrBi_2O_4 are also confirmed by EDX and XRD analysis. Under the irradiation from Xenon lamp (with UV-cutoff filter), tungsten lamp and ultraviolet lamp, the Orange II decolorization efficiency by photoelectrochemical oxidation is significantly higher than those by photocatalytic oxidation and electrochemical oxidation alone. Meanwhile, the synergetic effect under tungsten lamp irradiation is the most significant. Both the wavelength of the light source and the proportion between visible light and ultraviolet are proved to be fundamental for the photoelectrochemical process.

ACKNOWLEDGEMENTS

The authors would like to thank the financial support of the starting fund for talents of North China University of Water Resources and Electric Power and the National Science Foundation of China (Grant No. 50708037).

REFERENCES

- R. Andreozzi, V. Caprio, A. Insola and R. Marotta, *Catal. Today*, **53**, 51 (1999).
- S. Malato, P. Fernández-Ibáñez, M.I. Maldonado, J. Blanco and W. Gernjak, *Catal. Today*, **147**, 1 (2009).
- A. Yasar, N. Ahmad, H. Latif and A.A.A. Khan, *Ozone Sci. Eng.*, **29**, 485 (2007).
- C. Comminellis and G.H. Chen, *Electrochemistry for the Environment*. Springer Science Business Media, New York (2010).
- C. Comminellis, A. Kapalka, S. Malato, S.A. Parsons, I. Poullos and D. Mantzavinos, *J. Chem. Technol. Biotechnol.*, **83**, 769 (2008).
- R.T. Pelegrini, R.S. Freire, N. Duran and R. Bertazzoli, *Environ. Sci. Technol.*, **35**, 2849 (2001).
- J. Peller, O. Wiest and P.V. Kamat, *Environ. Sci. Technol.*, **37**, 1926 (2003).
- K. Vinodgopal, S. Hotchandani and P.V. Kamat, *J. Phys. Chem.*, **97**, 9040 (1993).
- Z.C. Wu and M.H. Zhou, *Environ. Sci. Technol.*, **35**, 2698 (2001).
- L.B. Stadler, A.S. Ernstoff, D.S. Aga and N.G. Love, *Environ. Sci. Technol.*, **46**, 10485 (2012).
- A.M. Polcaro, S. Palmas, F. Renoldi and M. Mascia, *J. Appl. Electrochem.*, **29**, 147 (1999).
- G.T. Li, J.H. Qu, X.W. Zhang and J.T. Ge, *Water Res.*, **40**, 213 (2006).
- C. Hu, X.X. Hu, J. Guo and J.H. Qu, *Environ. Sci. Technol.*, **40**, 5508 (2006).
- T. A. M. Haemers, D.J. W. Ijdo, *Mater. Res. Bull.*, **26**, 989 (1991).
- J.R. Feng and D.C. Johnson, *J. Electrochem. Soc.*, **138**, 3328 (1991).
- G.T. Li, H.Y. Yip, Ch. Hu and P.K. Wong, *Mater. Res. Bull.*, **46**, 153 (2011).
- X.Z. Li, H.L. Liu, P.T. Yue and Y.P. Sun, *Environ. Sci. Technol.*, **34**, 4401 (2000).
- S.P. Yu, Research of Photoelectric Catalytic Degradation of Organic Dyes, Doctor Dissertation of South China University of Technology (2004) (in Chinese).